AASLD
AMERICAN ASSOCIATION FOR
THE STUDY OF LIVER DISEASES

Ablation of high-mobility group box-1 in the liver reduces hepatocellular carcinoma but causes hyperbilirubinemia in Hippo signaling-deficient mice

Dipti Athavale[1] | Zhuolun Song[1] | Romain Desert[1] | Hui Han[1] |
Sukanta Das[1] | Xiaodong Ge[1] | Sai Santosh Babu Komakula[1] | Wei Chen[1] |
Shenglan Gao[1] | Daniel Lantvit[1] | Grace Guzman[1] | Natalia Nieto[1,2,3]

[1]Department of Pathology, University of Illinois at Chicago, Chicago, Illinois, USA

[2]Division of Gastroenterology and Hepatology, Department of Medicine, University of Illinois at Chicago, Chicago, Illinois, USA

[3]Research Biologist, Research & Development Service, Jesse Brown Veterans Affairs Medical Center, Chicago, Illinois, USA

Correspondence
Natalia Nieto, Department of Pathology, University of Illinois at Chicago, 840 S Wood St, Suite 130 CSN, MC 847, Chicago, IL 60612, USA.
Email: nnieto@uic.edu

Funding information
Supported by a U.S. Veterans Administration Grant from the Biomedical Laboratory Research & Development (I01BX005093) and Department of Pathology, University of Illinois at Chicago.

Abstract

Silencing the Hippo kinases mammalian sterile 20-like 1 and 2 (MST1/2) activates the transcriptional coactivator yes-associated protein (YAP) in human hepatocellular carcinoma (HCC). Hepatocyte-derived high-mobility group box-1 (HMGB1) regulates YAP expression; however, its contribution to HCC in the context of deregulated Hippo signaling is unknown. Here, we hypothesized that HMGB1 is required for hepatocarcinogenesis by activating YAP in Hippo signaling-deficient ($Mst1/2^{\Delta Hep}$) mice. $Mst1/2^{\Delta Hep}$ mice developed HCC within 3.5 months of age and had increased hepatic expression of HMGB1 and elevated YAP activity compared to controls. To understand the contribution of HMGB1, we generated $Mst1/2$&$Hmgb1^{\Delta Hep}$ mice. They exhibited decreased YAP activity, cell proliferation, inflammation, fibrosis, atypical ductal cell expansion, and HCC burden at 3.5 months compared to $Mst1/2^{\Delta Hep}$ mice. However, $Mst1/2$&$Hmgb1^{\Delta Hep}$ mice were smaller, developed hyperbilirubinemia, had more liver injury with intrahepatic biliary defects, and had reduced hemoglobin compared to $Mst1/2^{\Delta Hep}$ mice. *Conclusion:* Hepatic HMGB1 promotes hepatocarcinogenesis by regulation of YAP activity; nevertheless, it maintains intrahepatic bile duct physiology under Hippo signaling deficiency.

INTRODUCTION

Liver cancer is the second most common cause of cancer-related death worldwide,[1,2] and hepatocellular carcinoma (HCC) accounts for approximately 80% of the incidence of all liver cancers.[3] Current treatment options for HCC, such as surgical resection, liver transplantation, radiofrequency ablation, and transarterial chemoembolization, are curative for patients with early stage disease.[4] Unfortunately, most patients with HCC are not eligible for these therapeutic approaches due to late diagnosis and thus poor prognosis.[4] Targeted agents, such as sorafenib, regorafenib, nivolumab and lenvatinib, have proven to prolong survival in patients with HCC.[1] Nevertheless, novel therapeutic strategies are urgently needed due to the low chemotherapy sensitivity of HCC and the limited drugs available.

Hippo signaling is critical to control tissue growth; however, its tumor suppressor effects are reduced in approximately 30% of human HCCs.[5,6] When the Hippo signaling pathway is on, mammalian sterile 20-like 1 and 2 (MST1/2) and large tumor suppressor kinases 1/2 (LATS1/2) undergo phosphorylation. This leads to phosphorylation of the transcriptional coactivators yes-associated protein (YAP) and PDZ-binding motif (TAZ), preventing their translocation to the nucleus eventually undergo degradation.[7] Hepatic deletion of *Mst1/2* or overexpression of *Yap* promotes YAP translocation to the nucleus where it binds transcriptional enhancer factor domain (TEAD) family members and increases cell proliferation and progression to HCC or mixed HCC/cholangiocarcinoma between 3 and 4 months of age in mice.[7,8]

High-mobility group box-1 (HMGB1) is an architectural protein that binds the linker region of nucleosomal DNA, increases nucleosome instability, and facilitates nucleosome sliding. In addition, it bends promoter regions to enhance the interaction of transcription factors and is involved in DNA base excision repair and genome stability.[9] During liver injury, HMGB1 is passively released from hepatocytes as a result of necrosis and apoptosis or is actively secreted by inflammatory cells, acting as a sterile damage-associated molecular pattern.[10] In HCC, HMGB1 increases in tumor tissue compared to normal or adjacent nontumor tissue.[11] Importantly, the concentration of HMGB1 in serum correlates with tumor size, HCC stage, and grade.[12] In mice injected with diethylnitrosamine (DEN), HMGB1 is required for hepatocarcinogenesis; however, its role in regulating the Hippo signaling pathway and tumor progression is not completely understood. Ablation of *Hmgb1* in hepatocytes reduces tumor initiation by decreasing YAP expression and aerobic glycolysis but does not affect tumor progression.[13] In contrast, *Hmgb1*[ΔHep] mice treated with DEN and carbon tetrachloride show no difference in YAP protein or its target genes but have reduced hepatocarcinogenesis compared to controls.[14]

In this study, we hypothesized that HMGB1 accelerates HCC by activating YAP in Hippo signaling-deficient mice. We found that hepatic HMGB1 expression increases when ablating *Mst1/2* in the liver. Importantly, we demonstrated that deletion of *Hmgb1* in *Mst1/2*-deficient livers decreases YAP activity and HCC burden. However, HMGB1 is required to maintain intrahepatic bile duct (IHBD) physiology; therefore, when HMGB1 is ablated in the context of Hippo signaling deficiency, it causes hyperbilirubinemia and growth retardation.

MATERIALS AND METHODS

Mice

Albumin-Cre (*Alb*.Cre (B6.Cg-Speer6-ps1[Tg(Alb-cre)21Mgn]/J, JAX 003574)) mice were used as controls in all experiments. *Mst1/2*[floxed fl/fl] mice (*Stk4*[tm1.1Rjo]

Stk3[tm1.1Rjo]/J, JAX 017635) were obtained from the Jackson Laboratory (Bar Harbor, ME). The locus of X-over P1 (*loxP*) sites flank exons 4–5 and 5–6 of the serine/threonine protein kinase (*Stk*)4 and *Stk3* genes, respectively.[15] The *Hmgb1*[loxP] allele was created by inserting *loxP* sites within introns 1 and 2 and flanking exon 2 of *Hmgb1*.[16] The following breeding schemes were established to target these genes in the liver: (1) *Mst1/2*[fl/fl] mice were bred with *Alb*.Cre mice to generate *Mst1/2* knockout mice (*Mst1/2*[ΔHep]). (2) *Hmgb1*^{fl/fl} mice were bred with *Alb*.Cre mice to generate *Hmgb1* knockout mice (*Hmgb1*[ΔHep]). (3) *Mst1/2*[ΔHep] mice were bred with *Hmgb1*[ΔHep] mice to generate *Mst1/2&Hmgb1*[ΔHep] mice. Mice from both sexes were used in the study.

Study approval

All animals received humane care according to the criteria outlined in the Guide for the Care and Use of Laboratory Animals prepared by the National Academy of Sciences and published by the National Institutes of Health. Housing and husbandry conditions were approved by the University of Illinois at Chicago Institutional Animal Care and Use Committee before initiation of the studies. All *in vivo* experiments were carried out according to the Animal Research: Reporting of *In Vivo* Experiments guidelines.

Human data set analysis

UALCAN (http://ualcan.path.uab.edu) [17] was used to analyze the messenger RNA (mRNA) expression of *HMGB1* and *YAP1* in nontumor and tumor tissues in the human liver HCC data set from The Cancer Genome Atlas (TCGA). GEPIA (http://gepia.cancer-pku.cn) [18] was used to analyze the significance of the association between two transcripts in the same data set from the TCGA. Pearson's correlation was used to analyze a cohort of hepatitis B virus (HBV)-induced HCC and paired nontumor samples (GSE14520).

Biliary tree visualization

Injection of ink to visualize the biliary tree structures was performed as described.[19] Mice were sacrificed at 2 months of age, and livers were perfused with Hanks' balanced salt solution for 3 min at a flow rate of 5 ml/min. Undiluted waterproof ink (Higgins ink, #44032) was injected (15–30 µl) through the common bile duct until bile ducts on the liver surface were visible. After the ink injections, livers were harvested and stored in 10% buffered formalin for processing. To clear the tissue, fixed liver lobes were sequentially dehydrated in methanol in phosphate-buffered saline (50% and 80% for 1 hour) and in 100% methanol

overnight. They were then immersed in 2:1 benzyl benzoate:benzyl alcohol for 2 days.[20] Images were captured on an Olympus BX51 microscope (Tokyo, Japan).

Complete blood count

Blood was collected from the facial vein plexus in microtainer tubes with dipotassium ethylene diamine tetraacetic acid (K$_2$EDTA; BD Biosciences, NJ) at 2 months of age and was analyzed in a Siemens Advia 120 Hematology System (Erlangen, Germany) at the Biologic Resources Laboratory (University of Illinois at Chicago).

Statistics

Data are expressed as mean ± SEM. Statistical analysis between two groups was performed using the two-tailed Student t test. $p < 0.05$ was considered significant.

RESULTS

Mst1/2$^{\Delta Hep}$ mice show increased hepatic expression of HMGB1

To address whether Hippo signaling deficiency alters HMGB1 expression, we generated Mst1/2$^{\Delta Hep}$ mice and confirmed Mst1 and MST2 knockdown by quantitative real-time polymerase chain reaction (qPCR) and western blot, respectively (Figure S1). There was nuclear localization of YAP in hepatocytes and biliary epithelial cells (BECs) (Figure 1A) and increased mRNA of Yap and two of its target genes (cellular communication network factor 1 [Cyr61]) and connective tissue growth factor [Ctgf])[5,21] in Mst1/2$^{\Delta Hep}$ compared to control mice (Figure 1B), suggesting up-regulation of YAP activity. There was more HMGB1-positive staining in the nucleus of hepatocytes and BECs in Mst1/2$^{\Delta Hep}$ than in control mice (Figure 1C). This was further confirmed by qPCR (3-fold increase), western blot (2-fold increase), and enzyme-linked immunosorbent assay (8-fold increase in serum) in Mst1/2$^{\Delta Hep}$ compared to control mice at 3.5 months of age, when they already have HCC (Figure 1D,E; Figure S2). To rule out a potential contribution of HMGB1 from tumor tissue, protein expression was analyzed at 2 months of age before the development of tumors. We found a 1.3-fold increase in HMGB1 in Mst1/2$^{\Delta Hep}$ compared to control mice (Figure S3A). However, YAP protein expression remained similar at 2 and 3.5 months of age in the livers from Mst1/2$^{\Delta Hep}$ compared to control mice (Figure S3A,B). These results indicate that HMGB1 expression and YAP activity are increased in Hippo signaling-deficient mice.

Next, the HMGB1 and YAP1 mRNA levels and their correlation were analyzed in the human liver HCC cohort from the TCGA.[17,18] Both mRNAs increased in primary liver tumor tissues compared to normal controls, and there was positive correlation between the HMGB1 and YAP1 transcripts in tumor tissues (Figure 1F). Similar findings were obtained in the analysis of tumor and nontumor tissues from 247 patients with HBV-induced HCC (GSE14520). Notably, paired nontumor tissues showed strong positive correlation between the two transcripts (Figure 1G).

Ablation of Hmgb1 in Mst1/2$^{\Delta Hep}$ mice reduces tumor burden

To determine if HMGB1 in Mst1/2$^{\Delta Hep}$ mice is required for HCC, we generated additional control (Hmgb1$^{\Delta Hep}$) and triple knockout (Mst1/2&Hmgb1$^{\Delta Hep}$) mice and followed them for the development of tumors for 3.5 months. Ablation of Hmgb1 was confirmed by immunohistochemistry (IHC) (Figure S4A,B) and western blot (Figures S3A and S4C). Serum HMGB1 decreased in Mst1/2&Hmgb1$^{\Delta Hep}$ compared to Mst1/2$^{\Delta Hep}$ mice while it was elevated in Hmgb1$^{\Delta Hep}$ compared to control mice at 3.5 months, suggesting contribution from nonparenchymal cells (Figure S2). Both Mst1/2$^{\Delta Hep}$ and Mst1/2&Hmgb1$^{\Delta Hep}$ mice had higher liver weights and similar liver-to-body weight ratios than control or Hmgb1$^{\Delta Hep}$ mice; however, Mst1/2&Hmgb1$^{\Delta Hep}$ mice were thinner but had higher liver weight and liver-to-body weight ratio than control and Hmgb1$^{\Delta Hep}$ mice (Figure 2A).

Control and Hmgb1$^{\Delta Hep}$ mice did not develop tumors, while 100% (7 males and 5 females) of Mst1/2$^{\Delta Hep}$ and 78% (4 males and 3 females) of Mst1/2&Hmgb1$^{\Delta Hep}$ mice developed tumors at 3.5 months (Figure 2B). Macroscopic analysis indicated that Mst1/2&Hmgb1$^{\Delta Hep}$ mice had fewer and smaller tumors and reduced total tumor volume compared to Mst1/2$^{\Delta Hep}$ mice (Figure 2B,C). Histopathological evaluation of liver sections revealed multiple dysplastic nodules. The HCC growth patterns were pseudoglandular, solid, and trabecular (mostly grade II) in Mst1/2$^{\Delta Hep}$ and Mst1/2&Hmgb1$^{\Delta Hep}$ mice; however, the number of HCCs per mouse was significantly lower in Mst1/2&Hmgb1$^{\Delta Hep}$ compared to Mst1/2$^{\Delta Hep}$ mice (Figure 2C,D). These data suggest that HMGB1 promotes tumorigenesis in Mst1/2$^{\Delta Hep}$ mice.

Ablation of Hmgb1 in Mst1/2$^{\Delta Hep}$ mice decreases YAP activity and cell proliferation

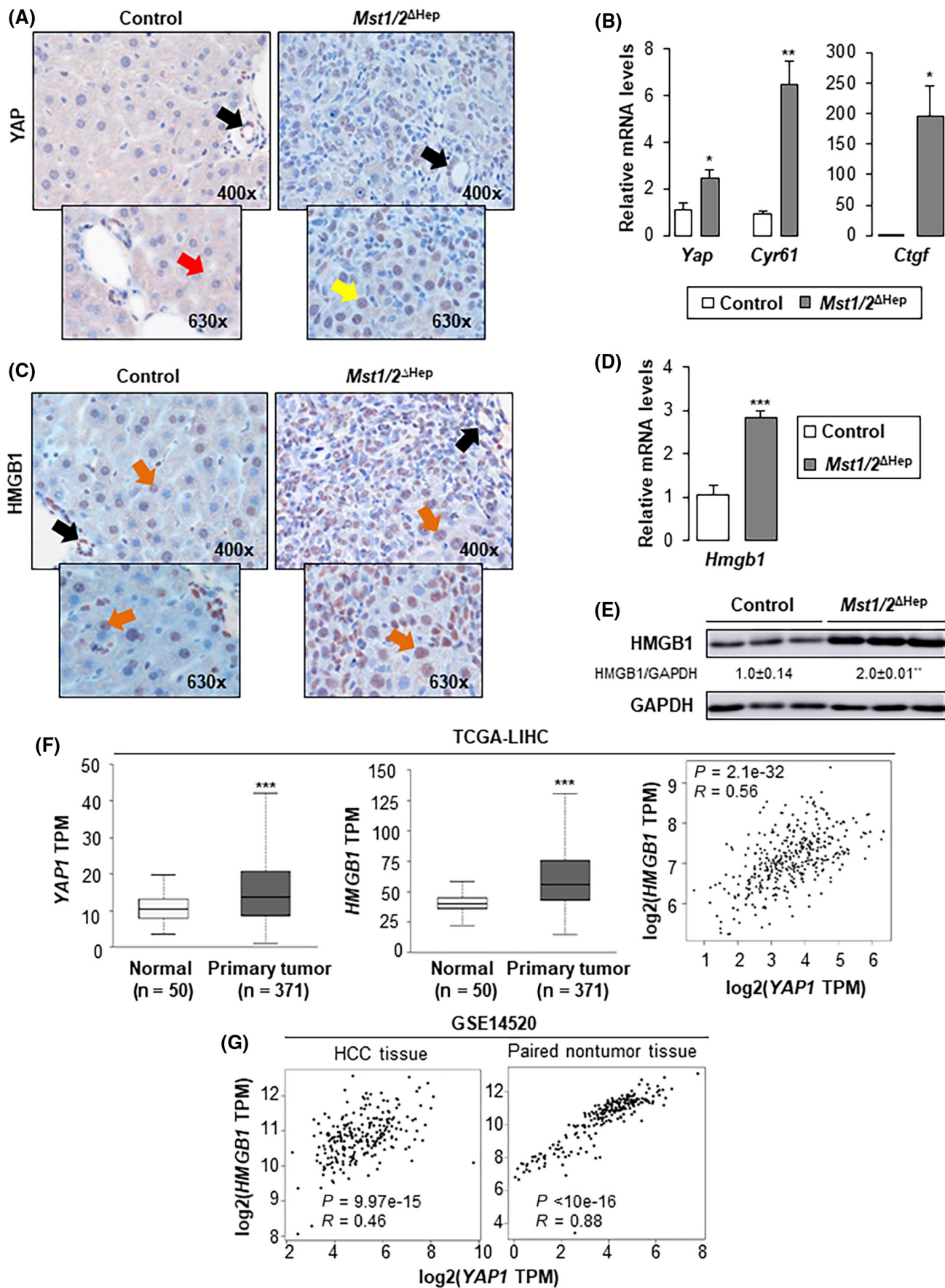A previous study demonstrated that deletion of hepatocyte-derived Hmgb1 decreases YAP gene

FIGURE 1 *Mst1/2*$^{\Delta Hep}$ mice show increased hepatic expression of HMGB1. Control and *Mst1/2*$^{\Delta Hep}$ mice were generated and followed for the development of tumors for 3.5 months. (A) YAP IHC in liver (red arrow shows cytoplasmic staining in hepatocytes; yellow arrow shows nuclear staining in hepatocytes; black arrows show nuclear staining in BECs). (B) Relative liver mRNA levels of *Yap*, *Cyr61*, and *Ctgf* (control n = 3; *Mst1/2*$^{\Delta Hep}$ n = 6). (C) HMGB1 IHC in liver (orange arrows show nuclear staining in hepatocytes; black arrow shows nuclear staining in BECs). (D) Relative liver mRNA levels of *Hmgb1* (control n = 3; *Mst1/2*$^{\Delta Hep}$ n = 6). (E) Western blot analysis of liver HMGB1 (n = 3/group). In A–E, values are given as mean ± SEM; *$p < 0.05$, **$p < 0.01$, ***$p < 0.001$ for *Mst1/2*$^{\Delta Hep}$ versus control. (F) Box plots of *YAP1* and *HMGB1* TPM in normal and HCC tissues from the human liver hepatocellular carcinoma (LIHC) cohort from the TCGA (left and middle panels). Graphs were obtained from UALCAN (http://ualcan.path.uab.edu), ***$p < 0.001$ for tumor versus normal. Spearman correlation analysis of *YAP1* and *HMGB1* obtained from GEPIA (http://gepia.cancer-pku.cn) (right panel). (G) Pearson correlation analysis of *YAP1* and *HMGB1* from a cohort of 247 patients with HBV-induced HCC with tumor and nontumor tissues (GSE14520). Abbreviations: BEC, biliary epithelial cell; *Ctgf*, connective tissue growth factor; *Cyr61*, cellular communication network factor 1; GAPDH, glyceraldehyde 3-phosphate dehydrogenase; HBV, hepatitis B virus; HCC, hepatocellular carcinoma; HMGB1, high-mobility group box-1; IHC, immunohistochemistry; LIHC, liver hepatocellular carcinoma; mRNA, messenger RNA; MST1/2, mammalian sterile 20-like 1 and 2; TCGA, The Cancer Genome Atlas; TPM, transcripts per million; *Yap*, yes-associated protein
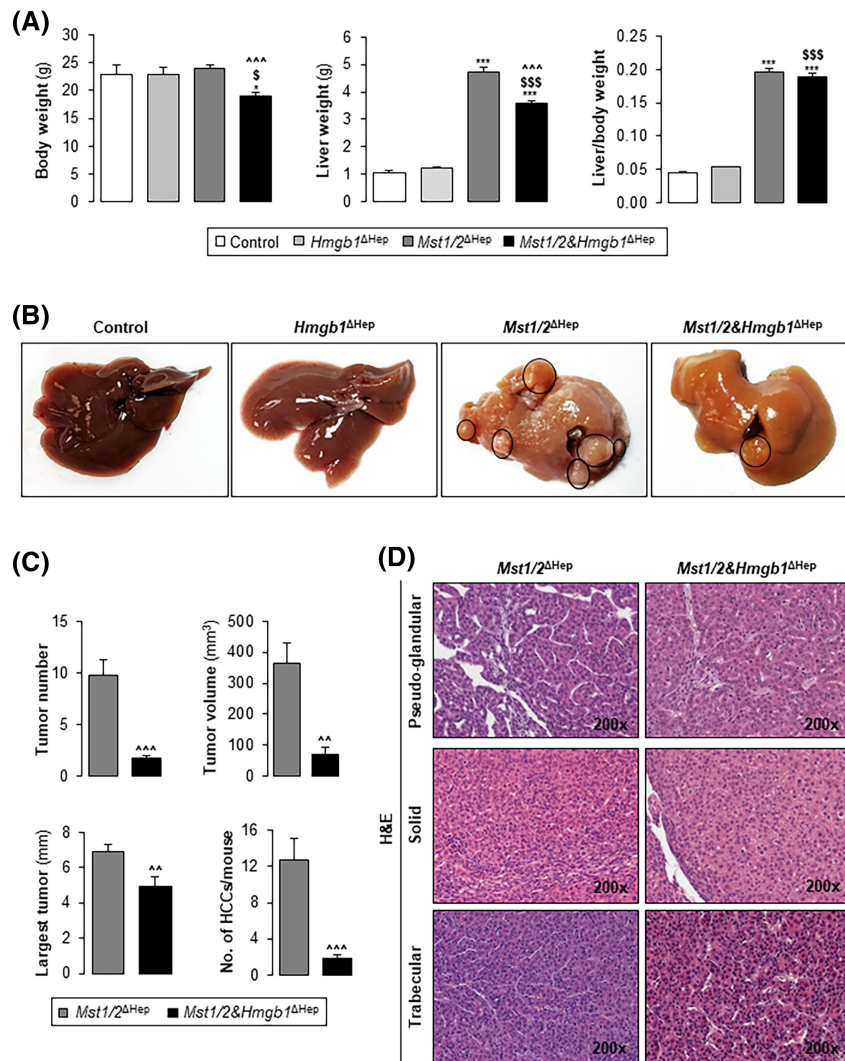

FIGURE 2 Ablation of *Hmgb1* in *Mst1/2*$^{\Delta Hep}$ mice reduces tumor burden. Control, *Hmgb1*$^{\Delta Hep}$, *Mst1/2*$^{\Delta Hep}$, and *Mst1/2&Hmgb1*$^{\Delta Hep}$ mice were generated and followed for the development of tumors for 3.5 months. (A) Body weight, liver weight, and liver-to-body weight ratio. (B) Macroscopic appearance of livers with tumors circled in black. (C) Tumor number, largest tumor diameter, total tumor volume, and number of HCCs/mouse. (D) H&E staining showing HCCs with pseudoglandular, solid, and trabecular growth patterns (control n = 6; *Hmgb1*$^{\Delta Hep}$ n = 5; *Mst1/2*$^{\Delta Hep}$ n = 12; *Mst1/2&Hmgb1*$^{\Delta Hep}$ n = 9). Values are given as mean ± SEM. *$p < 0.05$, ***$p < 0.001$ for *Mst1/2&Hmgb1*$^{\Delta Hep}$ or *Mst1/2*$^{\Delta Hep}$ versus control; $^{\$}p < 0.05$ and $^{\$\$\$}p < 0.001$ for *Mst1/2&Hmgb1*$^{\Delta Hep}$ versus *Hmgb1*$^{\Delta Hep}$; $^{\wedge\wedge}p < 0.01$ and $^{\wedge\wedge\wedge}p < 0.001$ for *Mst1/2&Hmgb1*$^{\Delta Hep}$ versus *Mst1/2*$^{\Delta Hep}$. Abbreviations: HCC, hepatocellular carcinoma; H&E, hematoxylin and eosin; HMGB1, high-mobility group box-1; MST1/2, mammalian sterile 20-like 1 and 2

expression.[13] Thus, we asked if the reduced HCC burden was associated with decreased YAP expression and activity in $Mst1/2\&Hmgb1^{\Delta Hep}$ mice. Yap mRNA decreased in $Mst1/2\&Hmgb1^{\Delta Hep}$ compared to $Mst1/2^{\Delta Hep}$ mice at 2 and 3.5 months (Figure 3A). This correlated with down-regulation of YAP target genes ($Ctgf$, $Cyr61$, and glypican-3 [$Gpc-3$]) and HCC markers ($Gpc-3$ and alpha fetoprotein [Afp]) in $Mst1/2\&Hmgb1^{\Delta Hep}$ compared to $Mst1/2^{\Delta Hep}$ mice (Figure 3A). Moreover, western blot analysis showed decreased GPC-3 in $Mst1/2\&Hmgb1^{\Delta Hep}$ compared to $Mst1/2^{\Delta Hep}$ mice at 3.5 months, suggesting that ablation of $Hmgb1$ decreases YAP activity (Figure 3B). GPC-3 protein was also detected in control and $Hmgb1^{\Delta Hep}$ whole-liver tissue lysates.[22] It has been reported that GA-binding protein alpha (GABPα) regulates Yap gene transcription and liver GABPα increases in $Mst1/2^{\Delta Hep}$ mice[23]; however in our model, GABPα expression in liver lysates at 2 months and in the nuclear fraction at 3.5 months remained similar in $Mst1/2\&Hmgb1^{\Delta Hep}$ and $Mst1/2^{\Delta Hep}$ mice (Figure S5A–C).

We further examined whether decreased Yap transcripts and activity correlated with down-regulation of YAP protein in $Mst1/2\&Hmgb1^{\Delta Hep}$ mice. Liver YAP protein expression remained similar in $Mst1/2\&Hmgb1^{\Delta Hep}$ and $Mst1/2^{\Delta Hep}$ mice at 2 and 3.5 months of age (Figure S3A,B). The Hippo pathway kinase cascade phosphorylates YAP in serine-127

and sequesters it in the cytoplasm for subsequent degradation.[7] Although not significant, we noted increased phosphorylated pYAP in $Mst1/2\&Hmgb1^{\Delta Hep}$ compared to $Mst1/2^{\Delta Hep}$ mice at 3.5 months (Figures S3B and S5A). Phosphorylation of LATS1/2, which triggers phosphorylation of YAP,[7] remained similar in $Mst1/2\&Hmgb1^{\Delta Hep}$ and $Mst1/2^{\Delta Hep}$ mice at 2 months (Figure S6A).

Next, we asked whether $Hmgb1$ ablation regulates YAP localization. IHC showed decreased YAP+ nuclei in $Mst1/2\&Hmgb1^{\Delta Hep}$ compared to $Mst1/2^{\Delta Hep}$ mice (Figure 4A). YAP was slightly reduced in the nuclear fraction from $Mst1/2\&Hmgb1^{\Delta Hep}$ compared to $Mst1/2^{\Delta Hep}$ mice at 3.5 months of age (Figure S5A). Importantly, mRNA of the YAP nuclear interactors $Tead1–4$ increased in $Mst1/2^{\Delta Hep}$ compared to control mice but decreased in $Mst1/2\&Hmgb1^{\Delta Hep}$ compared to $Mst1/2^{\Delta Hep}$ mice (Figure 4B). Overall, these findings indicate that ablation of $Hmgb1$ decreases YAP activity.

Because YAP activation promotes cell proliferation,[15] we analyzed markers of cell proliferation. Cyclin D1 (Ccnd1) mRNA, proliferating cell nuclear antigen (PCNA) expression, and Ki67 nuclear staining decreased in $Mst1/2\&Hmgb1^{\Delta Hep}$ compared to $Mst1/2^{\Delta Hep}$ mice at 2 and 3.5 months (Figures 3A and 4C; Figure S6A,B). To determine whether apoptosis was involved, we analyzed the cleavage of poly(adenosine diphosphate ribose) polymerase (PARP) and caspase-3; however, they were almost unchanged (Figure S6C).
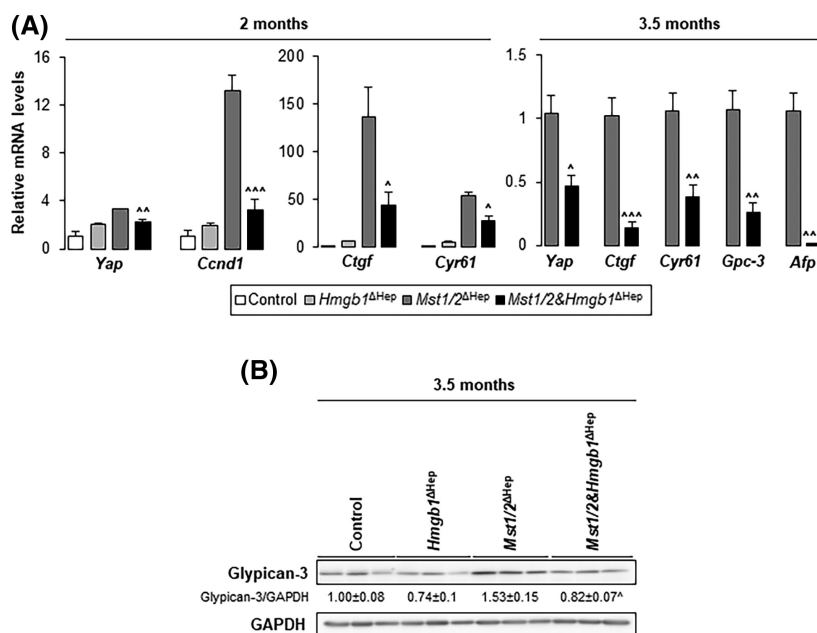

FIGURE 3 Ablation of $Hmgb1$ in $Mst1/2^{\Delta Hep}$ mice decreases YAP activity. Control, $Hmgb1^{\Delta Hep}$, $Mst1/2^{\Delta Hep}$, and $Mst1/2\&Hmgb1^{\Delta Hep}$ mice were generated and followed for the development of tumors for 2 or 3.5 months. (A) Relative liver mRNA levels of Yap, its targets ($Ctgf$, $Cyr61$, and $Gpc-3$), HCC markers ($Gpc-3$ and Afp), and $Ccnd1$ (n = 3–6/group). (B) Western blot analysis for liver GPC-3 at 3.5 months (n = 3/group). Values are given as mean ± SEM. $^p < 0.05$, $^{^^}p < 0.01$, $^{^^^}p < 0.001$ for $Mst1/2\&Hmgb1^{\Delta Hep}$ versus $Mst1/2^{\Delta Hep}$. Abbreviations: Afp, alpha fetoprotein; $Ccnd1$, cyclin D1; $Ctgf$, connective tissue growth factor; $Cyr61$, cellular communication network factor 1; GAPDH, glyceraldehyde 3-phosphate dehydrogenase; $Gpc-3$, glypican-3; HMGB1, high-mobility group box-1; mRNA, messenger RNA; MST1/2, mammalian sterile 20-like 1 and 2; Yap, yes-associated protein
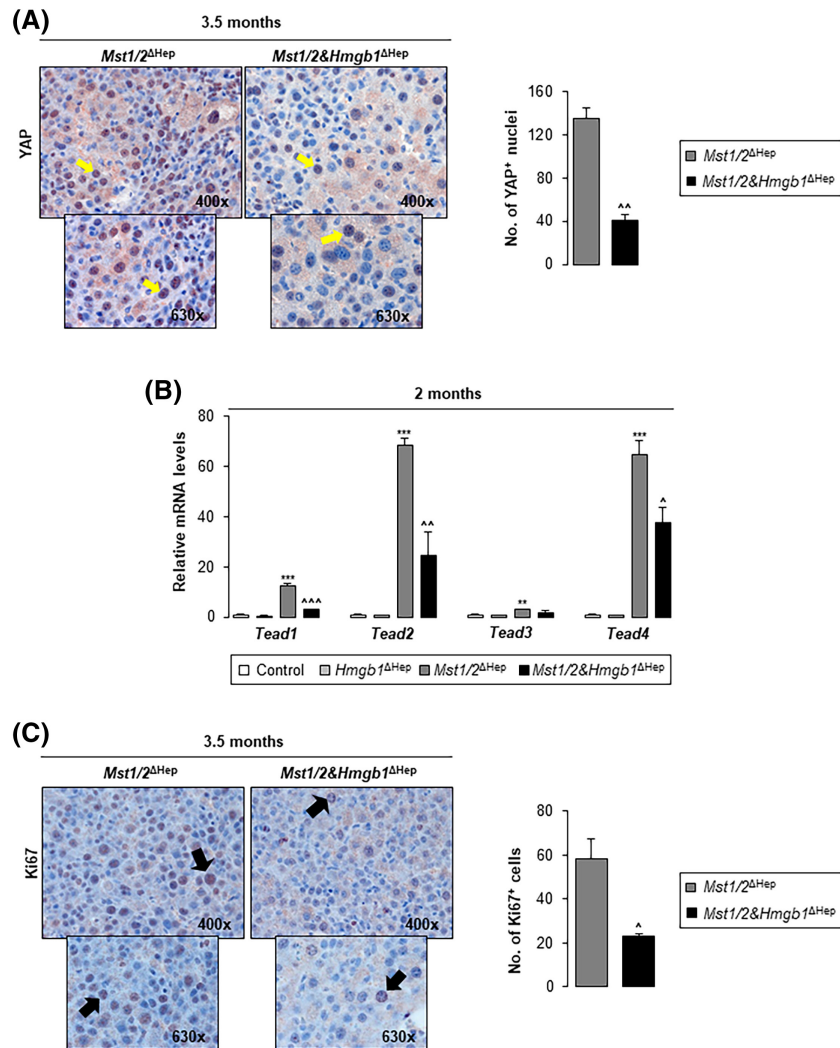
FIGURE 4 Ablation of *Hmgb1* in *Mst1/2*[ΔHep] mice decreases YAP[+] nuclei, *Tead* mRNAs, and proliferation. Control, *Hmgb1*[ΔHep], *Mst1/2*[ΔHep], and *Mst1/2&Hmgb1*[ΔHep] mice were generated and followed for the development of tumors for 2 or 3.5 months. (A) YAP IHC (yellow arrows show nuclear staining) (left) and quantification of the number of YAP^{+} cells in 10 fields at magnification ×200 (right) at 3.5 months (n = 3/group). (B) Relative liver mRNA levels of *Tead1–4* at 2 months (n = 3–4/group). (C) Ki67 IHC (black arrows show Ki67^{+} nuclei) (left) at 3.5 months and quantification of the number of Ki67^{+} cells in 10 fields at magnification ×200 (right) (n = 3/group). Values are given as mean ± SEM. **$p < 0.01$, ***$p < 0.001$ for *Mst1/2*[ΔHep] versus control. ^$p < 0.05$, ^^$p < 0.01$, ^^^$p < 0.001$ for *Mst1/2&Hmgb1*[ΔHep] versus *Mst1/2*[ΔHep]. Abbreviations: HMGB1, high-mobility group box-1; IHC, immunohistochemistry; mRNA, messenger RNA; MST1/2, mammalian sterile 20-like 1 and 2; *Tead*, transcriptional enhancer factor domain; YAP, yes-associated protein

Therefore, the livers from *Mst1/2&Hmgb1*[ΔHep] mice had decreased YAP activity and cell proliferation, both associated with reduced tumor burden, compared to *Mst1/2*[ΔHep] mice.

Ablation of *Hmgb1* in *Mst1/2*[ΔHep] mice reduces inflammation, fibrosis, and atypical ductal cell expansion

Mst1/2[ΔHep] mice have increased infiltration of macrophages and inflammation due to elevated YAP activity,[24] whereas overexpression of YAP activates myofibroblasts and promotes fibrosis.[21] Therefore,

we examined whether ablation of *Hmgb1* in *Mst1/2*[ΔHep] mice reduced inflammation and fibrosis. We found a decrease in mRNA of the proinflammatory cytokines interleukin-1β (*Il1β*) and C-C motif chemokine ligand 2 (*Ccl2*) in *Mst1/2&Hmgb1*[ΔHep] compared to *Mst1/2*[ΔHep] mice (Figure 5A). To evaluate whether there were less macrophages in the liver, we performed qPCR for adhesion G protein-coupled receptor E1 (*Adgre1*, F4/80) and integrin subunit alpha M (*Itgam*, CD11b) along with IHC for F4/80. *Mst1/2&Hmgb1*[ΔHep] had lower *Adgre1* and *Itgam* mRNAs and less F4/80^{+} cells (Figure 5A; Figure S7), indicating that HMGB1 reduces the number of macrophages in *Mst1/2*[ΔHep] mice.

(A)

(B)

(C)
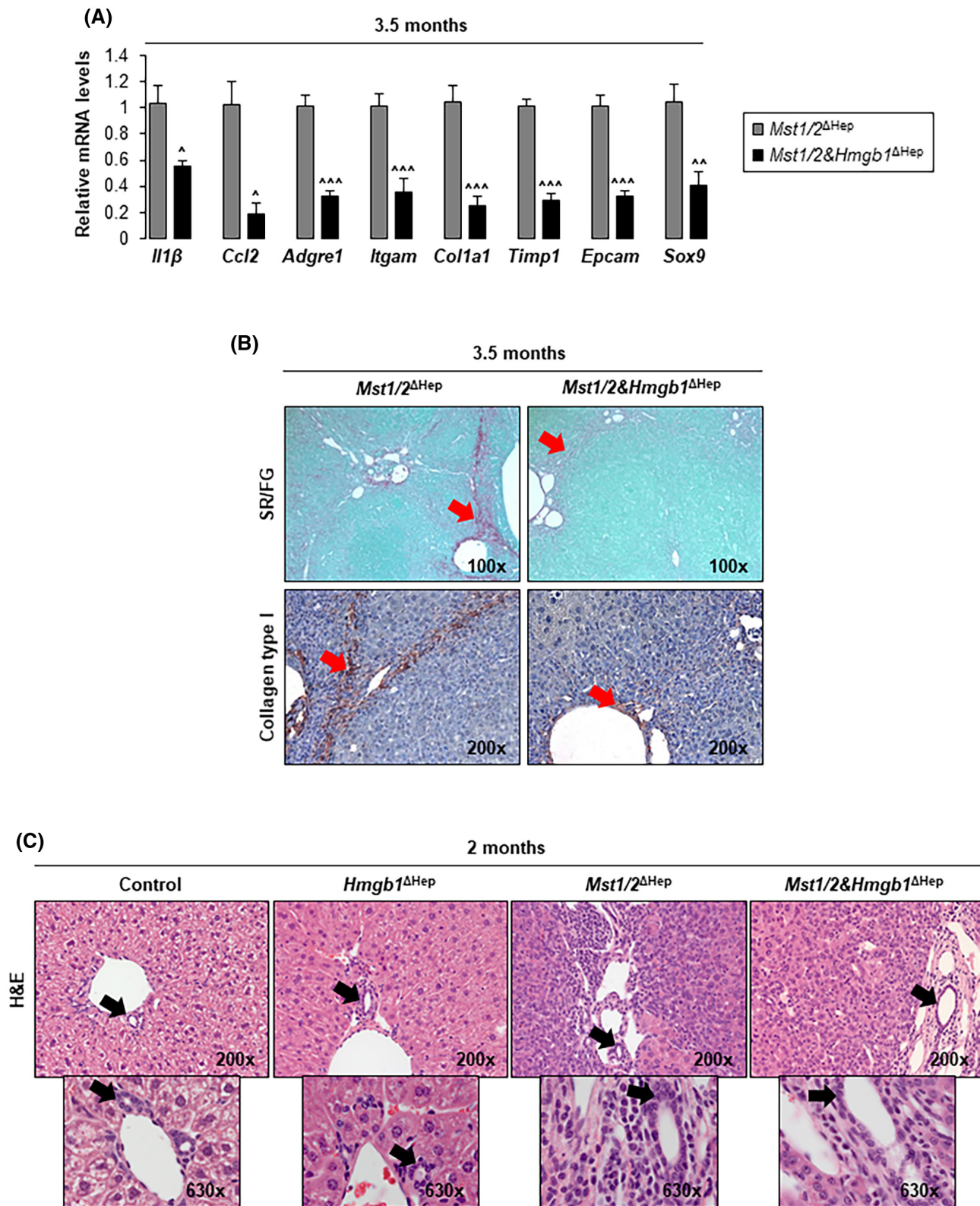
To determine the effect on fibrosis, we analyzed the mRNA expression of collagen type I alpha 1 chain (*Col1a1*) and tissue inhibitor of metalloproteinase 1 (*Timp1*), both of which decreased in *Mst1/2&Hmgb1*$^{\Delta Hep}$ compared to *Mst1/2*$^{\Delta Hep}$ mice (Figure 5A). In addition, sirius red/fast green staining for collagenous proteins and IHC for collagen type I revealed a major reduction in bridging and sinusoidal fibrosis in *Mst1/2&Hmgb1*$^{\Delta Hep}$ compared to *Mst1/2*$^{\Delta Hep}$ mice (Figure 5B).

Livers from *Mst1/2*$^{\Delta Hep}$ mice showed proliferative atypical ductal cells (ADCs), which infiltrate the liver parenchyma by 2 months and surround hepatic plates

FIGURE 5 Ablation of *Hmgb1* in *Mst1/2*$^{\Delta Hep}$ mice reduces inflammation, fibrosis, and ADCs. Control, *Hmgb1*$^{\Delta Hep}$, *Mst1/2*$^{\Delta Hep}$, and *Mst1/2&Hmgb1*$^{\Delta Hep}$ mice were generated and followed for the development of tumors for 2 or 3.5 months. (A) Relative liver mRNA levels of *Il1β*, *Ccl2*, *Adgre1*, *Itgam*, *Col1a1*, *Timp1*, *Epcam*, and *Sox9* at 3.5 months (n = 3–6/group). (B) Sirius red/fast green staining (top) and collagen type I IHC (bottom) (red arrows show collagen deposits) at 3.5 months. (C) H&E staining at 2 months. Images show zone 1 (black arrows show anatomical BDs) with expansion of ADCs (small round cells with scant cytoplasm) in *Mst1/2*$^{\Delta Hep}$ and *Mst1/2&Hmgb1*$^{\Delta Hep}$ mice. Values are given as mean ± SEM. ^$p < 0.05$, ^^$p < 0.01$, ^^^$p < 0.001$ for *Mst1/2&Hmgb1*$^{\Delta Hep}$ versus *Mst1/2*$^{\Delta Hep}$. Abbreviations: ADC, atypical ductal cell; *Adgre1*, adhesion G protein-coupled receptor E1; BD, bile duct; *Ccl2*, C-C motif chemokine ligand 2; *Col1a1*, collagen type I alpha 1 chain; *Epcam*, epithelial cell adhesion molecule; H&E, hematoxylin and eosin; HMGB1, high-mobility group box-1; IHC, immunohistochemistry; *Il1β*, interleukin-1β; *Itgam*, integrin subunit alpha M; mRNA, messenger RNA; MST1/2, mammalian sterile 20-like 1 and 2; *Sox9*, sex-determining region Y-box 9; SR/FG, sirius red/fast green; *Timp1*, tissue inhibitor of metalloproteinase 1

by 3 months of age.[15,25] Thus, we evaluated whether *Hmgb1* deficiency reduces ADCs. Hematoxylin and eosin staining of livers from 2-month-old *Mst1/2*$^{\Delta Hep}$ mice showed more expansion of ADCs (small round cells with scant cytoplasm) in portal areas than in *Mst1/2&Hmgb1*$^{\Delta Hep}$ mice (Figure 5C). In support of this, the mRNA of sex-determining region Y-box 9 (*Sox;* a marker for ADCs) and of epithelial cell adhesion molecule (*Epcam*; a marker of ductal/progenitor cells) decreased in *Mst1/2&Hmgb1*$^{\Delta Hep}$ compared to *Mst1/2*$^{\Delta Hep}$ mice at 3.5 months of age (Figure 5A). Moreover, the expression of SOX9 increased in 2-month-old *Mst1/2*$^{\Delta Hep}$ mice compared to controls, in which the staining was restricted to ductal cells, but decreased in *Mst1/2&Hmgb1*$^{\Delta Hep}$ compared to *Mst1/2*$^{\Delta Hep}$ mice (Figure 6A; Figure S8A), which was also validated by western blot (Figure 6B).

We then asked if ADCs express HMGB1 and contribute to the increase in HMGB1 protein in *Mst1/2*$^{\Delta Hep}$ mice. HMGB1 colocalized with SOX9$^+$ cells in *Mst1/2*$^{\Delta Hep}$ but not in *Mst1/2&Hmgb1*$^{\Delta Hep}$ mice (Figure 6C). Importantly, *SOX9* positively correlated with *YAP1* and *HMGB1* mRNAs in the human liver HCC cohort from the TCGA (Figure S8B). Taken together, these results suggest that ablation of *Hmgb1* lowers inflammation, fibrosis, and SOX9$^+$-ADC expansion in *Mst1/2&Hmgb1*$^{\Delta Hep}$ compared to *Mst1/2*$^{\Delta Hep}$ mice, contributing to reduce HCC.

Mst1/2&Hmgb1$^{\Delta Hep}$ mice develop hyperbilirubinemia

Although tumor burden was reduced in *Mst1/2& Hmgb1*$^{\Delta Hep}$ mice, they were smaller, more lethargic, and had increased liver injury shown by elevated serum alanine aminotransferase activity compared to age-matched *Mst1/2*$^{\Delta Hep}$ mice (Figures 2A and 7A,B). Because the serum from *Mst1/2&Hmgb1*$^{\Delta Hep}$ mice was jaundiced (Figure S9A), we measured the concentration of bilirubin. Concentrations of total and conjugated bilirubin were significantly higher in *Mst1/2&Hmgb1*$^{\Delta Hep}$ compared to the other three groups of mice (Figure 7C). To assess if *Mst1/2&Hmgb1*$^{\Delta Hep}$ mice had altered bilirubin import, conjugation, or export,[26] we analyzed the mRNA levels of adenosine triphosphate-binding

cassette subfamily C members 2/3 (*Abcc2/3*), uridine diphosphoglucuronate glucuronosyltransferase family 1 member A1 (*Ugt1a1*), and organic anion-transporting polypeptide 1B1/B3 (*Oatp1b1/3*); however, the levels remained similar in *Mst1/2&Hmgb1*$^{\Delta Hep}$ and *Mst1/2*$^{\Delta Hep}$ mice except for *Oatp1b1/b3*, which decreased in *Mst1/2&Hmgb1*$^{\Delta Hep}$ compared to *Mst1/2*$^{\Delta Hep}$ mice (Figure S9B).

IHBD developmental defects and paucity are associated with jaundice in mice.[27,28] Therefore, we evaluated the IHBD network by injecting ink through the common bile duct (BD). Control and *Hmgb1*$^{\Delta Hep}$ mice showed a well-formed biliary tree network in which the branches reached the liver periphery. *Mst1/2*$^{\Delta Hep}$ mice showed many small branches (hypertrophy) compared to controls, while ink-filled branches in *Mst1/2&Hmgb1*$^{\Delta Hep}$ mice were dilated and did not reach the liver margin (Figure 7D). BDs were enlarged with flattened and disoriented epithelial cells in *Mst1/2&Hmgb1*$^{\Delta Hep}$ mice at 2 months (Figures 5C and 6A; Figure S8A). Moreover, *Mst1/2&Hmgb1*$^{\Delta Hep}$ mice showed foci of feathery degeneration, the classic morphologic manifestation of cholestatic-induced hepatocyte injury that is characterized by swollen, pale-staining, and finely vacuolated hepatocytes (Figure S9C). Because Notch signaling regulates IHBD development and is activated in *Mst1/2*$^{\Delta Hep}$ mice,[5,25] we evaluated if ablation of *Hmgb1* affected Notch signaling. qPCR analysis revealed that the Notch ligand jagged-1 (*Jag1*), and its targets (Hes family BHLH transcription factor 1 [*Hes1*] and Notch-regulated ankyrin repeat protein [*Nrarp*]) decreased in *Mst1/2&Hmgb1*$^{\Delta Hep}$ compared to *Mst1/2*$^{\Delta Hep}$ mice (Figure S10).

Hemoglobin from damaged red blood cells (RBCs) is catabolized to bilirubin by phagocytes in the spleen, liver, and bone marrow.[29] The increase in total bilirubin in *Mst1/2&Hmgb1*$^{\Delta Hep}$ mice prompted us to measure the concentration of hemoglobin and perform blood cell counts. At 2 months of age, *Mst1/2&Hmgb1*$^{\Delta Hep}$ mice had less hemoglobin, hematocrit, mean corpuscular volume, and mean corpuscular hemoglobin but increased serum lactate dehydrogenase (LDH) activity compared to *Mst1/2*$^{\Delta Hep}$ mice (Table S1; Figures S11 and S12A). Because iron produced from heme degradation is recycled for erythropoiesis,[20] we measured the concentration of iron in serum. *Mst1/2&Hmgb1*$^{\Delta Hep}$
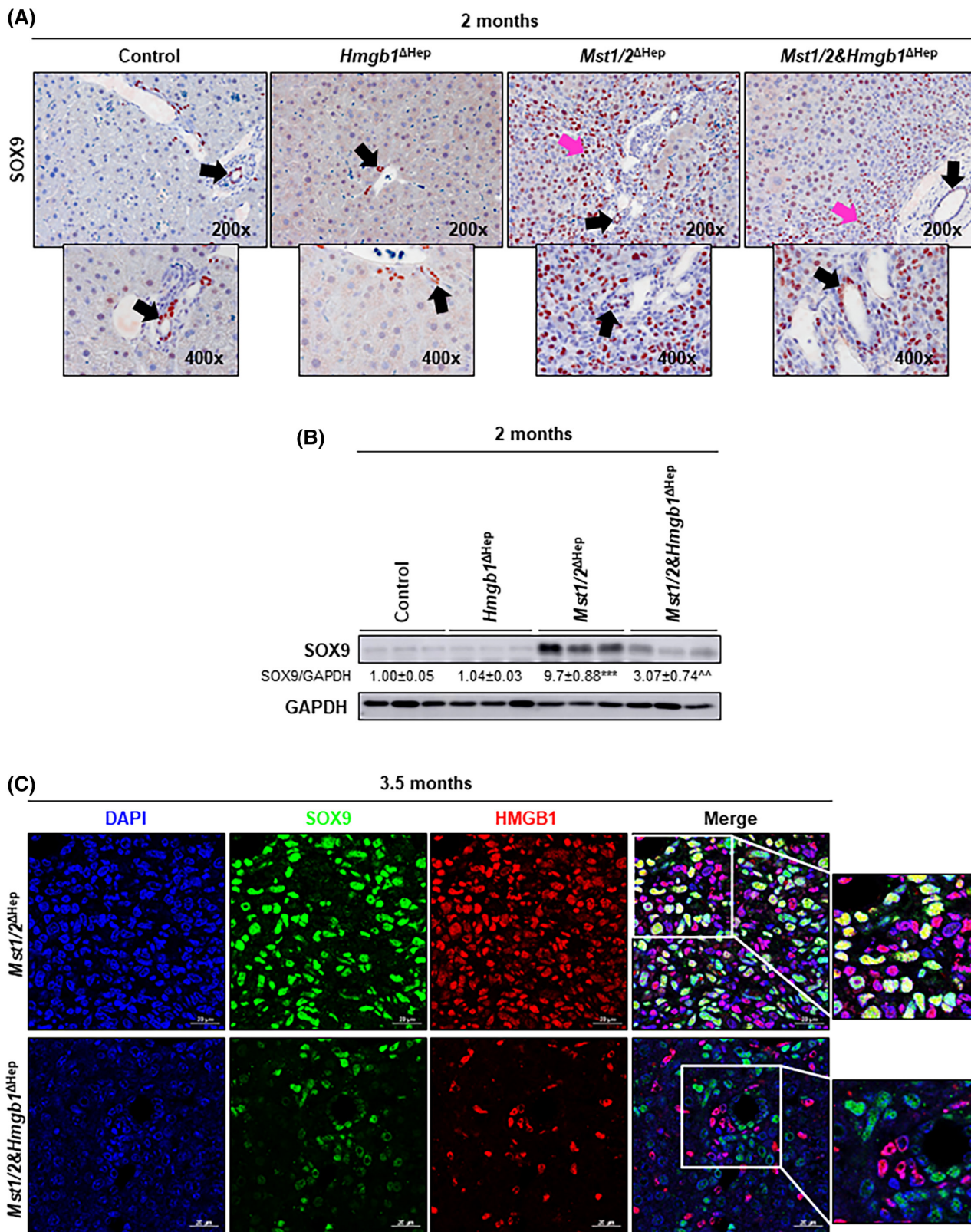
FIGURE 6 Ablation of *Hmgb1* in *Mst1/2*$^{\Delta Hep}$ mice reduces SOX9$^+$ ADCs. Control, *Hmgb1*$^{\Delta Hep}$, *Mst1/2*$^{\Delta Hep}$, and *Mst1/2&Hmgb1*$^{\Delta Hep}$ mice were generated and followed for the development of tumors for 2 or 3.5 months. (A) SOX9 IHC at 2 months (black arrows show staining in anatomical BDs; pink arrows show staining in ADCs). (B) Western blot analysis of liver SOX9 at 2 months. (C) Immunofluorescence showing colocalization of DAPI (blue), SOX9 (green), and HMGB1 (red) (magnification ×630). Scale bar, 20 μm. Values are given as mean ± SEM. ***$p < 0.001$ for *Mst1/2*$^{\Delta Hep}$ versus control; ^^$p < 0.01$ for *Mst1/2&Hmgb1*$^{\Delta Hep}$ versus *Mst1/2*$^{\Delta Hep}$. Abbreviations: ADC, atypical ductal cell; BD, bile duct; DAPI, 4′,6-diamidino-2-phenylindole; GAPDH, glyceraldehyde 3-phosphate dehydrogenase; HMGB1, high-mobility group box-1; IHC, immunohistochemistry; MST1/2, mammalian sterile 20-like 1 and 2; Sox9, sex-determining region Y-box 9
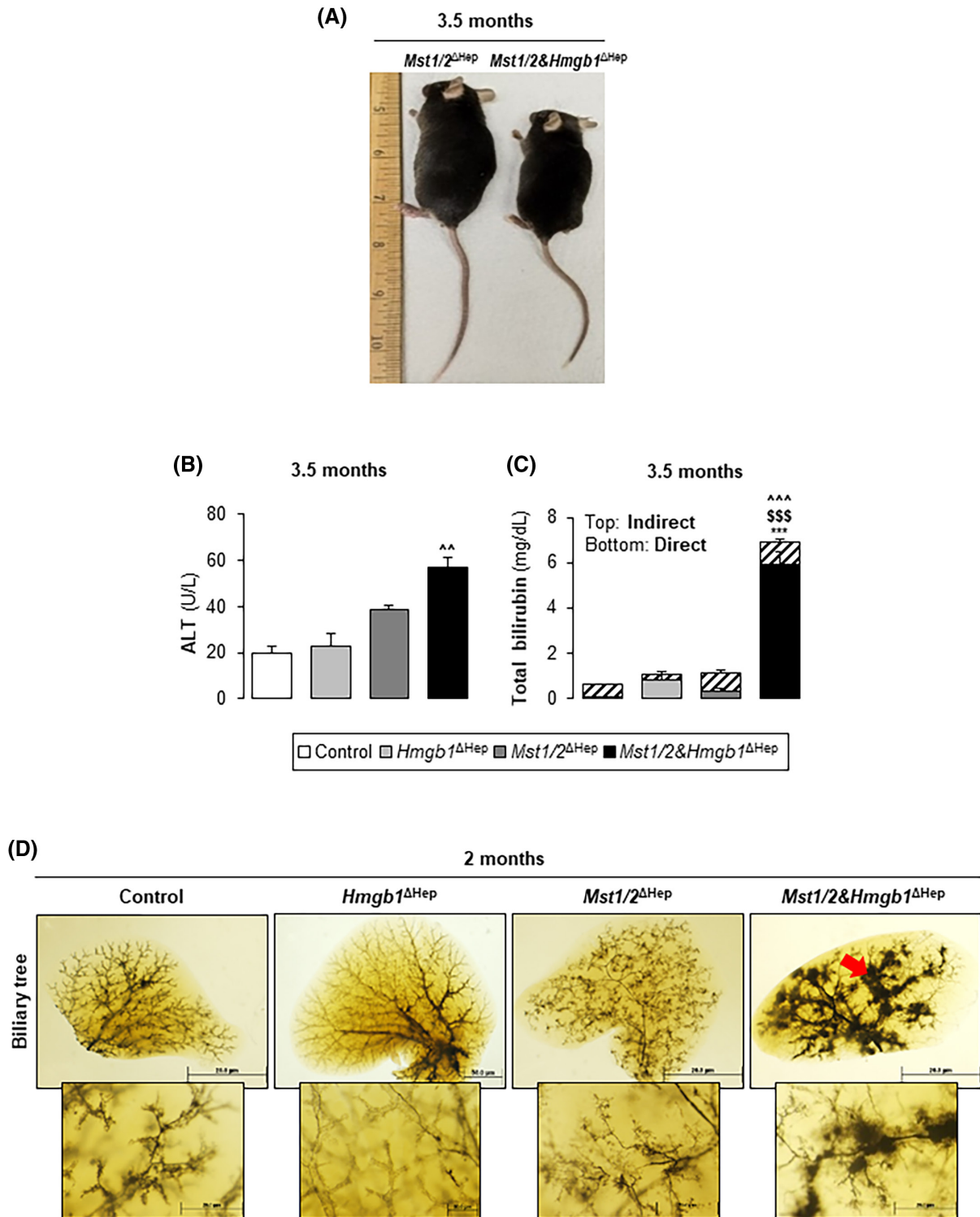
FIGURE 7 Ablation of *Hmgb1* in *Mst1/2*$^{\Delta Hep}$ mice induces hyperbilirubinemia. Control, *Hmgb1*$^{\Delta Hep}$, *Mst1/2*$^{\Delta Hep}$, and *Mst1/2&Hmgb1*$^{\Delta Hep}$ mice were generated and followed for the development of tumors for 2 or 3.5 months. (A) Mouse size at 3.5 months. (B) Serum ALT activity at 3.5 months. (C) Total serum bilirubin (direct and indirect) at 3.5 months. In B,C, control n = 4; *Hmgb1*$^{\Delta Hep}$ n = 4; *Mst1/2*$^{\Delta Hep}$ n = 5; *Mst1/2&Hmgb1*$^{\Delta Hep}$ n = 5. (D) Ink-stained IHBD tree at 2 months (red arrow shows abnormal ink distribution) (control n = 3; *Hmgb1*$^{\Delta Hep}$ n = 2; *Mst1/2*$^{\Delta Hep}$ n = 5; *Mst1/2&Hmgb1*$^{\Delta Hep}$ n = 3) (magnification ×0.8 top and ×4 bottom). Scale bar, 20 μm. Values are given as mean ± SEM. ***$p < 0.001$ for *Mst1/2&Hmgb1*$^{\Delta Hep}$ versus control; $^{\$\$\$}p < 0.001$ for *Mst1/2&Hmgb1*$^{\Delta Hep}$ versus *Hmgb1*$^{\Delta Hep}$; ^^$p < 0.01$, ^^^$p < 0.001$ for *Mst1/2&Hmgb1*$^{\Delta Hep}$ versus *Mst1/2*$^{\Delta Hep}$. Abbreviations: ALT, alanine aminotransferase; HMGB1, high-mobility group box-1; IHBD, intrahepatic bile duct; MST1/2, mammalian sterile 20-like 1 and 2

had reduced serum iron at 2 and 3.5 months of age and elevated iron staining in the spleen at 3.5 months compared to $Mst1/2^{\Delta Hep}$ mice (Figure S12B,C). The systemic iron concentration regulator hepcidin (*Hamp*) was increased in $Mst1/2\&Hmgb1^{\Delta Hep}$ compared to $Mst1/2^{\Delta Hep}$ mice (Figure S12D). These data indicate that decreased Notch signaling, abnormal IHBD physiology, and reduced hemoglobin are associated with hyperbilirubinemia in $Mst1/2\&Hmgb1^{\Delta Hep}$ mice.

DISCUSSION

In this study, we demonstrated that HMGB1 and the Hippo signaling pathway participate in HCC as $Mst1/2^{\Delta Hep}$ showed significant increase in HMGB1 mRNA and protein compared to control mice while ablation of *Hmgb1* reduced tumor burden. Because YAP is activated in $Mst1/2^{\Delta Hep}$ mice,[8] we considered that it could increase HMGB1 expression by a feedback mechanism. However, mice with hepatocyte-specific deletion of *Yap* and *Taz* do not show changes in HMGB1 expression compared to controls,[21] and knockdown of *Yap* with short hairpin RNA in HCC cell lines does not reduce HMGB1.[13] Therefore, these studies suggest that YAP may not affect HMGB1 expression, although it could be regulated by a yet unexplored mechanism in $Mst1/2^{\Delta Hep}$ mice.

However, we showed that HMGB1 affects *Yap* because *Yap* mRNA decreased in $Mst1/2\&Hmgb1^{\Delta Hep}$ compared to $Mst1/2^{\Delta Hep}$ mice. An earlier study demonstrated that GABPα transcriptionally regulates *Yap*[23] and is increased in $Mst1/2^{\Delta Hep}$ mice. While GABPα increased in liver from $Mst1/2^{\Delta Hep}$ compared to controls, it did not decrease in $Mst1/2\&Hmgb1^{\Delta Hep}$ compared to $Mst1/2^{\Delta Hep}$ mice at 2 months while *Yap* transcription was down-regulated. Furthermore, nuclear GABPα remained similar in $Mst1/2\&Hmgb1^{\Delta Hep}$ and $Mst1/2^{\Delta Hep}$ mice at 3.5 months. Because HMGB1 and GABPα interact with each other and with the promoter of *Yap* to increase activity,[13] we considered that *Hmgb1* ablation could reduce *Yap* transactivation*;* nonetheless, the decrease in *Yap* transcription did not correlate with the decrease in YAP translation as the expression remained unchanged in both groups of mice at 2 and 3.5 months of age.

Based on the increase in pYAP, the decrease in YAP$^+$ nuclei and the parallel decrease in YAP target genes in $Mst1/2\&Hmgb1^{\Delta Hep}$ compared to $Mst1/2^{\Delta Hep}$ mice, we concluded that *Hmgb1* deletion decreases YAP activity rather than its expression under Hippo signaling deficiency. Increased cell proliferation, inflammation, oval/DC expansion, and fibrosis, all linked to higher YAP activity,[13,21,24,30] decreased in $Mst1/2\&Hmgb1^{\Delta Hep}$ compared to $Mst1/2^{\Delta Hep}$ mice. Because $Mst1/2\&Hmgb1^{\Delta Hep}$ mice showed lower *Tead1*, *Tead2*, and *Tead4* mRNAs,

this likely limits the interaction of YAP with TEAD and hence reduces YAP activity and HCC.

Although HCC initiation and progression were delayed by *Hmgb1* deficiency, $Mst1/2\&Hmgb1^{\Delta Hep}$ mice had higher liver weight, PCNA staining, and *Ccnd1* mRNA than control and $Hmgb1^{\Delta Hep}$ mice, suggesting active cell proliferation and possibly that the rate of oncogenesis does not correspond with the rate of cell proliferation. *Hmgb1* ablation did not decrease all YAP-active cells or completely block YAP activity in $Mst1/2\&Hmgb1^{\Delta Hep}$ livers, suggesting that remnant YAP activity is associated with increased proliferation in $Mst1/2\&Hmgb1^{\Delta Hep}$ compared to control and $Hmgb1^{\Delta Hep}$ livers.

Loss of Hippo signaling and hepatocyte-specific overexpression of YAP expands ADCs to reach approximately 80% of the total liver mass compared to controls.[25,30] ADCs are positive for hepatic progenitor (HPC)/DC markers, such as SOX9, EpCAM, and pan-cytokeratin, and originate mainly from dedifferentiation of hepatocytes with YAP activation.[25,30] Accordingly, there was a major increase in SOX9$^+$ ADCs in $Mst1/2^{\Delta Hep}$ mice compared to controls but were reduced in $Mst1/2\&Hmgb1^{\Delta Hep}$ mice. Expansion of SOX9$^+$ ADCs and colocalization of HMGB1 with SOX9 provides a clue for the overall increase in HMGB1 expression in $Mst1/2^{\Delta Hep}$ mice compared to controls. This suggests that HMGB1 is required for proliferation of ADCs or dedifferentiation of hepatocytes into ADCs; hence, *Hmgb1* ablation reduces this effect. Indeed, in autophagy-deficient livers or in mice fed with a 3,5-diethoxycarbonyl-1,4-dihydrocollidine (DDC)/choline-deficient diet, which induces ductular reaction with proliferation of HPCs and DCs, ablation of *Hmgb1* completely abolished SOX9- and EpCAM-positive HPCs/DCs.[31] Moreover, *Yap* deletion in hepatocytes and BECs decreases ductular reaction and SOX9$^+$ proliferative cells in the DDC model.[32] These reports along with our observations indicate that the HMGB1–Hippo/YAP axis is key for expansion of ADCs or HPC/DCs and is worth further investigation as it is relevant for liver repair and regeneration.[33]

Epcam, *Sox9*, and *Afp*, a progenitor and oncofetal signature associated with worse HCC prognosis,[34–36] were down-regulated in $Mst1/2\&Hmgb1^{\Delta Hep}$ compared to $Mst1/2^{\Delta Hep}$ mice. The *Sox9* promoter has TEAD4-binding sites and is a direct transcriptional target of the YAP/TEAD complex.[25,37] SOX9 expression increases in HCC,[38] and patients with HCC with high SOX9 expression have reduced overall survival.[39] SOX9 induces sorafenib resistance in experimental models of HCC.[40] We showed increased expression and colocalization of SOX9 with HMGB1 in $Mst1/2^{\Delta Hep}$ mice together with a positive correlation between *HMGB1* and *SOX9* and between *YAP1* and *SOX9* in the liver HCC cohort from the TCGA, indicating that SOX9 could be a key molecular target of the HMGB1–YAP axis.

The IHBD developmental defects, such as hyperbilirubinemia, feathery degeneration, and growth retardation, observed in *Mst1/2&Hmgb1*^{ΔHep} mice were reported in mice with ablation of *Yap* in hepatoblasts and of *Notch* in hepatocytes.[41,42] Injecting newborn mice with an inhibitor of the Notch pathway hampered the elongation of the luminal network of IHBDs, precluding them from reaching the liver periphery.[43] The Hippo pathway functions through Notch signaling as *Notch2* is a direct transcriptional target of YAP and regulates IHBD development in mice.[25,44] We did not observe complete loss of the IHBD tree, but dilation of BDs and uneven ink distribution toward the liver margin along with reduced Notch pathway genes in *Mst1/2&Hmgb1*^{ΔHep} mice at 2 months, suggesting that elongation of small BDs is affected. These results underscore the importance of studying the biological functions of the HMGB1–YAP–Notch axis in embryonic and early postnatal development of the intrahepatic biliary system under Hippo pathway deficiency.

Despite a reduced tumor burden, *Mst1/2&Hmgb1*^{ΔHep} mice were morbid, had growth retardation, and hyperbilirubinemia. In the context of *Mst1/2* loss, we believe that reduced HCC development and hyperbilirubinemia represent two different aspects of the biological roles of HMGB1. Because *Alb*.Cre targets hepatocytes and BECs,[42] it is possible that *Hmgb1* ablation in hepatocytes mediates the antitumor effect while ablation in BECs alters biliary homeostasis under Hippo deficiency. Future studies targeting HMGB1 with small interfering RNA lipid nanoparticles in *Mst1/2*^{ΔHep} mice at postnatal stages (when IHBD development is complete[42]) could elucidate the therapeutic potential of *Hmgb1* inhibition in YAP-driven HCCs as well as highlight the adverse biliary effects, if any.

Elevated levels of conjugated bilirubin cause RBC death and anemia in mice with BD ligation.[45] We observed increased conjugated bilirubin and LDH activity in *Mst1/2&Hmgb1*^{ΔHep} mice, suggesting RBC death.[46] Hemolysis releases hemoglobin that is converted to bilirubin. Impaired IHBD physiology limits bilirubin excretion, causing hyperbilirubinemia, and further enhances RBC lysis, as observed in *Mst1/2&Hmgb1*^{ΔHep} mice. An unaltered RBC count combined with an elevated percentage of reticulocytes suggests increased erythrocyte turnover.[45] *Mst1/2&Hmgb1*^{ΔHep} mice had a reduced concentration of iron in serum but increased iron deposits in spleen. The liver maintains the systemic iron homeostasis by producing transferrin, ferritin and hepcidin.[47] Hepcidin is an iron regulatory hormone that blocks the only iron exporter, ferroportin (FPN), thus limiting the systemic concentration of iron.[47,48] The increased expression of hepcidin in *Mst1/2&Hmgb1*^{ΔHep} mice suggests that it could block FPN and prevent iron mobilization to the blood.

Therefore, the HMGB1–Hippo/YAP axis may be critical for iron homeostasis in the liver.

In conclusion, our findings demonstrate that HMGB1 promotes HCC progression and regulates YAP activity, cell proliferation, inflammation, and fibrosis but also controls serum bilirubin concentration by maintaining intrahepatic biliary physiology in Hippo signaling-deficient mice.

CONFLICT OF INTEREST
The authors have no conflict of interest.

AUTHOR CONTRIBUTIONS
Dipti Athavale carried out the experiments and wrote the manuscript with support from Zhuolun Song, Romain Desert, Hui Han, Sukanta Das, Xiaodong Ge, Sai Santosh Babu Komakula, Wei Chen, Shenglan Gao, and Natalia Nieto. Zhuolun Song and Daniel Lantvit helped with breeding mice and performing experiments. Xiaodong Ge and Grace Guzman supervised the scoring of the slides. Natalia Nieto supervised the project and obtained funding.

ORCID
Zhuolun Song https://orcid.org/0000-0001-5101-3950
Natalia Nieto https://orcid.org/0000-0002-7941-6804

REFERENCES
1. Forner A, Reig M, Bruix J. Hepatocellular carcinoma. Lancet. 2018;391:1301–14.
2. Edge SB, Compton CC. The American Joint Committee on Cancer: the 7th edition of the AJCC cancer staging manual and the future of TNM. Ann Surg Oncol. 2010;17:1471–4.
3. Bray F, Ferlay J, Soerjomataram I, Siegel RL, Torre LA, Jemal A. Global cancer statistics 2018: GLOBOCAN estimates of incidence and mortality worldwide for 36 cancers in 185 countries. CA Cancer J Clin. 2018;68:394–424. Erratum in: CA Cancer J Clin. 2020;70:313.
4. El-Serag HB, Marrero JA, Rudolph L, Reddy KR. Diagnosis and treatment of hepatocellular carcinoma. Gastroenterology. 2008;134:1752–63.
5. Kim W, Khan SK, Gvozdenovic-Jeremic J, Kim Y, Dahlman J, Kim H, et al. Hippo signaling interactions with Wnt/beta-catenin and Notch signaling repress liver tumorigenesis. J Clin Invest. 2017;127:137–52.
6. Perra A, Kowalik MA, Ghiso E, Ledda-Columbano GM, Di Tommaso L, Angioni MM, et al. YAP activation is an early event and a potential therapeutic target in liver cancer development. J Hepatol. 2014;61:1088–96.

7. Song H, Mak KK, Topol L, Yun K, Hu J, Garrett L, et al. Mammalian Mst1 and Mst2 kinases play essential roles in organ size control and tumor suppression. Proc Natl Acad Sci U S A. 2010;107:1431–6.

8. Zhou D, Conrad C, Xia F, Park JS, Payer B, Yin Y, et al. Mst1 and Mst2 maintain hepatocyte quiescence and suppress hepatocellular carcinoma development through inactivation of the Yap1 oncogene. Cancer Cell. 2009;16:425–38.

9. Kang R, Chen R, Zhang Q, Hou W, Wu S, Cao L, et al. HMGB1 in health and disease. Mol Aspects Med. 2014;40:1–116.

10. Gaskell H, Ge X, Nieto N. High-mobility group box-1 and liver disease. Hepatol Commun. 2018;2:1005–20.

11. Zhang LU, Han J, Wu H, Liang X, Zhang J, Li J, et al. The association of HMGB1 expression with clinicopathological significance and prognosis in hepatocellular carcinoma: a meta-analysis and literature review. PLoS One. 2014;9: e110626.

12. Zhou RR, Kuang XY, Huang Y, Li N, Zou MX, Tang DL, et al. Potential role of high mobility group box 1 in hepatocellular carcinoma. Cell Adh Migr. 2014;8:493–8.

13. Chen R, Zhu S, Fan X-G, Wang H, Lotze MT, Zeh HJ, et al. High mobility group protein B1 controls liver cancer initiation through yes-associated protein -dependent aerobic glycolysis. Hepatology. 2018;67:1823–41.

14. Hernandez C, Huebener P, Pradere JP, Antoine DJ, Friedman RA, Schwabe RF. HMGB1 links chronic liver injury to progenitor responses and hepatocarcinogenesis. J Clin Invest. 2018;128:2436–51. Erratum in: J Clin Invest. 2019;129:1803.

15. Lu LI, Li Y, Kim SM, Bossuyt W, Liu PU, Qiu Q, et al. Hippo signaling is a potent in vivo growth and tumor suppressor pathway in the mammalian liver. Proc Natl Acad Sci U S A. 2010;107:1437–42.

16. Huang H, Nace GW, McDonald K-A, Tai S, Klune JR, Rosborough BR, et al. Hepatocyte-specific high-mobility group box 1 deletion worsens the injury in liver ischemia/reperfusion: a role for intracellular high-mobility group box 1 in cellular protection. Hepatology. 2014;59:1984–97.

17. Chandrashekar DS, Bashel B, Balasubramanya SAH, Creighton CJ, Ponce-Rodriguez I, Chakravarthi B, et al. UALCAN: a portal for facilitating tumor subgroup gene expression and survival analyses. Neoplasia. 2017;19:649–58.

18. Tang Z, Li C, Kang B, Gao G, Li C, Zhang Z. GEPIA: a web server for cancer and normal gene expression profiling and interactive analyses. Nucleic Acids Res. 2017;45:W98–102.

19. Schaub JR, Huppert KA, Kurial SNT, Hsu BY, Cast AE, Donnelly B, et al. De novo formation of the biliary system by TGFbeta-mediated hepatocyte transdifferentiation. Nature. 2018;557:247–51.

20. Kaneko K, Kamimoto K, Miyajima A, Itoh T. Adaptive remodeling of the biliary architecture underlies liver homeostasis. Hepatology. 2015;61:2056–66.

21. Mooring M, Fowl BH, Lum SZC, Liu YE, Yao K, Softic S, et al. Hepatocyte stress increases expression of yes-associated protein and transcriptional coactivator with PDZ-binding motif in hepatocytes to promote parenchymal inflammation and fibrosis. Hepatology. 2020;71:1813–30.

22. Grozdanov PN, Yovchev MI, Dabeva MD. The oncofetal protein glypican-3 is a novel marker of hepatic progenitor/oval cells. Lab Invest. 2006;86:1272–84.

23. Wu H, Xiao Y, Zhang S, Ji S, Wei L, Fan F, et al. The Ets transcription factor GABP is a component of the Hippo pathway essential for growth and antioxidant defense. Cell Rep. 2013;3:1663–77.

24. Kim W, Khan SK, Liu Y, Xu R, Park O, He Y, et al. Hepatic Hippo signaling inhibits protumoural microenvironment to suppress hepatocellular carcinoma. Gut. 2018;67:1692–703.

25. Yimlamai D, Christodoulou C, Galli G, Yanger K, Pepe-Mooney B, Gurung B, et al. Hippo pathway activity influences liver cell fate. Cell. 2014;157:1324–38.

26. Keppler D. The roles of MRP2, MRP3, OATP1B1, and OATP1B3 in conjugated hyperbilirubinemia. Drug Metab Dispos. 2014;42: 561–5.

27. Geisler F, Strazzabosco M. Emerging roles of Notch signaling in liver disease. Hepatology. 2015;61:382–92.

28. Zhang N, Bai H, David KK, Dong J, Zheng Y, Cai J, et al. The Merlin/NF2 tumor suppressor functions through the YAP oncoprotein to regulate tissue homeostasis in mammals. Dev Cell. 2010;19:27–38.

29. Vitek L. Bilirubin as a signaling molecule. Med Res Rev. 2020;40:1335–51.

30. Lee K-P, Lee J-H, Kim T-S, Kim T-H, Park H-D, Byun J-S, et al. The Hippo-Salvador pathway restrains hepatic oval cell proliferation, liver size, and liver tumorigenesis. Proc Natl Acad Sci U S A. 2010;107:8248–53.

31. Khambu B, Huda N, Chen X, Antoine DJ, Li Y, Dai G, et al. HMGB1 promotes ductular reaction and tumorigenesis in autophagy-deficient livers. J Clin Invest. 2019;129:2163.

32. Planas-Paz L, Sun T, Pikiolek M, Cochran NR, Bergling S, Orsini V, et al. YAP, but not RSPO-LGR4/5, signaling in biliary epithelial cells promotes a ductular reaction in response to liver injury. Cell Stem Cell. 2019;25:39–53.e10.

33. Miyajima A, Tanaka M, Itoh T. Stem/progenitor cells in liver development, homeostasis, regeneration, and reprogramming. Cell Stem Cell. 2014;14:561–74.

34. Lee J-S, Heo J, Libbrecht L, Chu I-S, Kaposi-Novak P, Calvisi DF, et al. A novel prognostic subtype of human hepatocellular carcinoma derived from hepatic progenitor cells. Nat Med. 2006;12:410–6.

35. Yamashita T, Forgues M, Wang W, Kim JW, Ye Q, Jia H, et al. EpCAM and alpha-fetoprotein expression defines novel prognostic subtypes of hepatocellular carcinoma. Cancer Res. 2008;68:1451–61.

36. Yang X-R, Xu Y, Yu B, Zhou J, Qiu S-J, Shi G-M, et al. High expression levels of putative hepatic stem/progenitor cell biomarkers related to tumour angiogenesis and poor prognosis of hepatocellular carcinoma. Gut. 2010;59:953–62.

37. Wang L, Zhang Z, Yu X, Huang X, Liu Z, Chai Y, et al. Unbalanced YAP-SOX9 circuit drives stemness and malignant progression in esophageal squamous cell carcinoma. Oncogene. 2019;38:2042–55.

38. Grimm D, Bauer J, Wise P, Krüger M, Simonsen U, Wehland M, et al. The role of SOX family members in solid tumours and metastasis. Semin Cancer Biol. 2020;67:122–53.

39. Liu C, Liu L, Chen X, Cheng J, Zhang H, Shen J, et al. Sox9 regulates self-renewal and tumorigenicity by promoting symmetrical cell division of cancer stem cells in hepatocellular carcinoma. Hepatology. 2016;64:117–29.

40. Wang M, Wang Z, Zhi X, Ding W, Xiong J, Tao T, et al. SOX9 enhances sorafenib resistance through upregulating ABCG2 expression in hepatocellular carcinoma. Biomed Pharmacother. 2020;129:110315.

41. Geisler F, Nagl F, Mazur PK, Lee M, Zimber-Strobl U, Strobl LJ, et al. Liver-specific inactivation of Notch2, but not Notch1, compromises intrahepatic bile duct development in mice. Hepatology. 2008;48:607–16.

42. Molina LM, Zhu J, Li Q, Pradhan-Sundd T, Krutsenko Y, Sayed K, et al. Compensatory hepatic adaptation accompanies permanent absence of intrahepatic biliary network due to YAP1 loss in liver progenitors. Cell Rep. 2021;36:109310.

43. Tanimizu N, Kaneko K, Itoh T, Ichinohe N, Ishii M, Mizuguchi T, et al. Intrahepatic bile ducts are developed through formation of homogeneous continuous luminal network and its dynamic rearrangement in mice. Hepatology. 2016;64:175–88.

44. Wu N, Nguyen Q, Wan Y, Zhou T, Venter J, Frampton GA, et al. The Hippo signaling functions through the Notch signaling to regulate intrahepatic bile duct development in mammals. Lab Invest. 2017;97:843–53.

45. Lang E, Gatidis S, Freise NF, Bock H, Kubitz R, Lauermann C, et al. Conjugated bilirubin triggers anemia by inducing erythrocyte death. Hepatology. 2015;61:275–84.

46. Kato GJ, McGowan V, Machado RF, Little JA, Taylor J, Morris CR, et al. Lactate dehydrogenase as a biomarker of hemolysis-associated nitric oxide resistance, priapism, leg ulceration, pulmonary hypertension, and death in patients with sickle cell disease. Blood. 2006;107:2279–85.

47. Rishi G, Subramaniam VN. The liver in regulation of iron homeostasis. Am J Physiol Gastrointest Liver Physiol. 2017;313:G157–65.

48. Pagani A, Nai A, Silvestri L, Camaschella C. Hepcidin and anemia: a tight relationship. Front Physiol. 2019;10:1294.

SUPPORTING INFORMATION

Additional supporting information may be found in the online version of the article at the publisher's website.